

Synthesis of CuInSe₂ Nanocrystals with Trigonal Pyramidal Shape

Bonil Koo, Reken N. Patel, and Brian A. Korgel*

Department of Chemical Engineering, Center for Nano- and Molecular Science and Technology, and Texas Materials Institute, The University of Texas at Austin, Austin, Texas 78712-1062

Received October 13, 2008; E-mail: korgel@che.utexas.edu

Semiconductor nanocrystals are interesting candidates as new light-absorbing materials for photovoltaic devices (PVs).^{1–5} They can be dispersed in solvents and deposited at low temperature on various substrates, including plastics,^{1,2} mixed with polymers to make hybrid light-absorbing layers,³ or infiltrated as dye replacements in sensitized mesoporous TiO₂ or ZnO films.^{4,5} Many different nanocrystals can be synthesized with optical gaps at the red edge of the solar spectrum, including CdTe,⁶ PbSe,⁷ Ge,⁸ Si,⁹ and I–III–VI₂ chalcopyrite compounds such as CuInS₂, CuInSe₂, and Cu(In_xGa_{1–x})Se₂.^{10–19} The I–III–VI₂ chalcopyrite nanocrystals are particularly interesting because of their high absorption coefficients, good photostability, and demonstrated high PV efficiency from vapor deposited films.²⁰

This communication reports a new synthetic route to monodisperse, solution-stable chalcopyrite CuInSe₂ nanocrystals. Central to the synthesis is the use of selenourea as a Se source, oleylamine as a coordinating solvent, and careful control over the reaction temperature and the way that reactants are combined. Furthermore, these nanocrystals exhibit an interesting trigonal pyramidal shape that arises from the polarity of the surface facets.

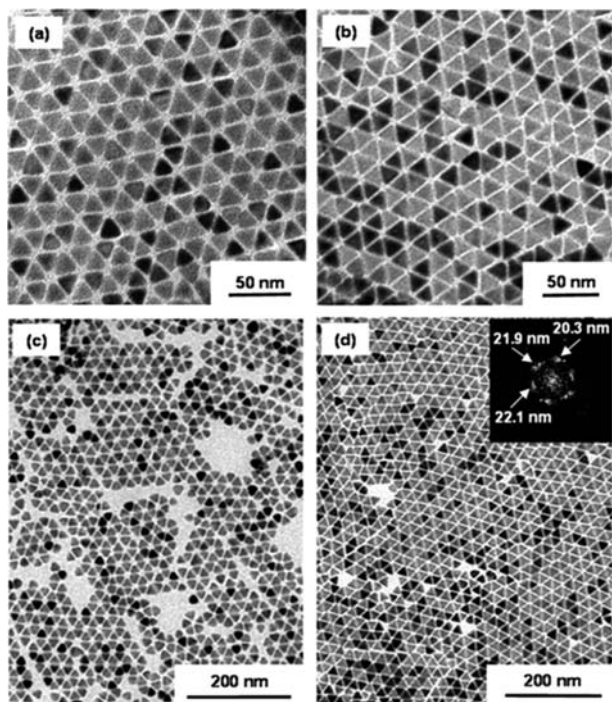
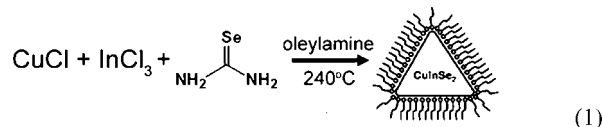


Figure 1. TEM images of CuInSe₂ nanocrystals. The nanocrystals in (a) and (c) have an average length of 16.1 nm on two sides and 16.9 nm on the other side, and the nanocrystals in (b) and (d) have an average length of 16.4 nm on two sides and 17.5 nm on the other side. The fast Fourier transform (FFT) of the nanocrystals in (d) (in the inset) reveals positional order in the monolayer.

Figure 1 shows TEM images of nanocrystals obtained from reaction 1. The nanocrystals are triangular in shape and monodisperse.



The precise ways in which reactants are combined and the temperature is manipulated are critical to obtaining monodisperse nanocrystals. InCl₃ and CuCl were first combined under air-free conditions in oleylamine and heated to 130 °C. Selenourea was added after the temperature was decreased to 100 °C. The reaction mixture was then heated to 240 °C and held there for 1 h.

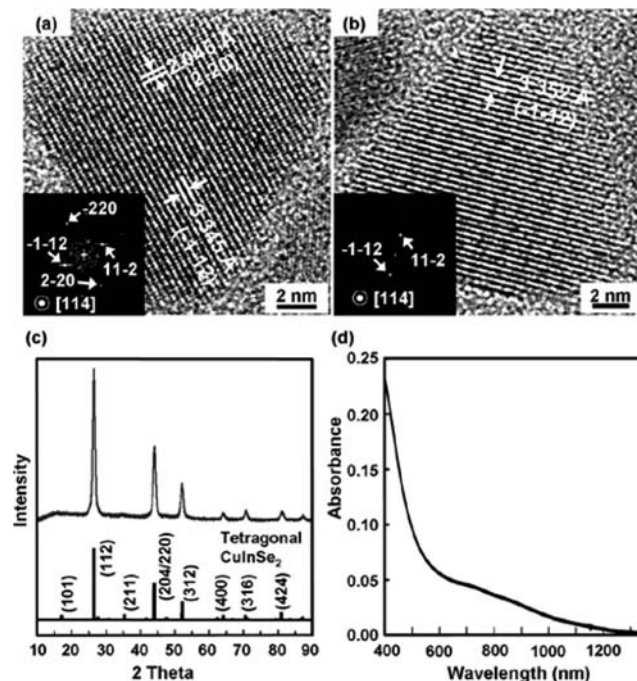


Figure 2. (a, b) TEM images of CuInSe₂ nanocrystals. The FFTs in the insets in (a) and (b) index to chalcopyrite CuInSe₂. The measured *d*-spacings of 3.35 and 2.05 Å respectively correspond to the {112} and {220} lattice planes of tetragonal (chalcopyrite) CuInSe₂ (3.351 and 2.046 Å). (c) XRD pattern ($\lambda = 1.54$ Å) for the CuInSe₂ nanocrystals. The stick pattern for chalcopyrite (tetragonal) CuInSe₂ (JCPDS No. 40-1487) is provided for reference. (d) Room-temperature UV–vis absorbance spectrum of an optically clear dispersion of CuInSe₂ nanocrystals in chloroform. See the Supporting Information for experimental details.

X-ray diffraction (XRD) (Figure 2c) and energy dispersive X-ray spectroscopy (EDS) (see the Supporting Information) confirmed that the nanocrystal composition is chalcopyrite (tetragonal) CuInSe₂. The optical gap of 1 eV measured by absorbance

spectroscopy (Figure 2d) is also consistent with chalcopyrite CuInSe_2 .²¹ In the TEM images, lattice fringes corresponding to the $\{112\}$ and $\{220\}$ chalcopyrite CuInSe_2 planes were predominantly visible. In fact, nanocrystals imaged by TEM generally had a common crystallographic orientation with respect to the substrate. For example, the nanocrystals in Figure 2a,b are both viewed down the $[114]$ zone axis, and the $(\bar{1}\bar{1}2)$ and $(2\bar{2}0)$ lattice planes are visible and oriented in the same way with respect to the triangular structure of the nanocrystals. Scanning electron microscopy (SEM) revealed that the nanocrystals have a trigonal pyramidal shape (see the Supporting Information). On the basis of this shape and the crystallographic orientations observed by TEM, the crystallographic model of the CuInSe_2 nanocrystals in Figure 3a was formulated: the nanocrystals are bounded by three $\{114\}$ and one $(\bar{1}\bar{1}2)$ surface facets. The nanocrystals in Figure 2a,b, for example, are on (114) facets, and the base of the trigonal pyramid (oriented perpendicular to the substrate) is a $(\bar{1}\bar{1}2)$ plane. The other top exposed surface facets are most likely $(\bar{1}\bar{1}4)$ and $(1\bar{1}4)$ planes.

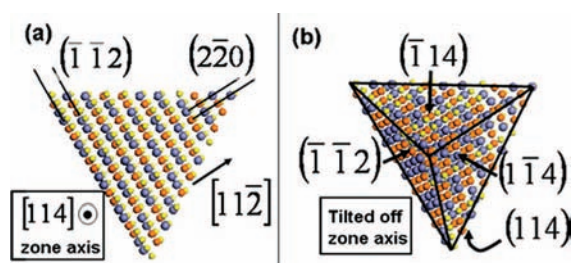


Figure 3. Crystallographic models of the trigonal pyramidal-shaped CuInSe_2 nanocrystals. The nanocrystal in (a) is viewed down the $[114]$ zone axis, like the nanocrystals imaged by TEM in Figure 2, and the nanocrystal portrayed in (b) is viewed slightly off the $[114]$ zone axis to illustrate the three-dimensional shape of the nanocrystal and its $(\bar{1}\bar{1}2)$, (114) , and $(1\bar{1}4)$ surface facets.

The nanocrystal shape appears to be related to the surface-facet polarity: the (112) and (114) chalcopyrite planes are structurally equivalent to the (111) and (112) planes of a cubic sphalerite crystal and are polar and nonpolar surfaces, respectively (see the Supporting Information). The surface-facet polarity and stability determine the nanocrystal shape, as in other nanocrystal materials studied in the recent past, including nanorods, trigonal pyramidal CdS , CdSe , and CdTe ,^{22–32} and disk-shaped Cu_2S ³³ and CuS .³⁴ The CuInSe_2 nanocrystals form with a relatively stable cation- or anion-terminated $(\bar{1}\bar{1}2)$ surface facet and an opposing (112) surface that is correspondingly unstable and leads to fast growth in the $[11\bar{2}]$ direction. The three other nonpolar $\{114\}$ sidewall facets are relatively stable surfaces. The other nonpolar surfaces of chalcopyrite CuInSe_2 —the (110) surfaces—are not observed. These observations are consistent with what is known about CuInSe_2 crystal surfaces.^{35,36}

Oleylamine underlies the nanocrystal synthesis, providing a solvating medium for CuCl and InCl_3 and serving as an effective capping ligand. However, when nanocrystals were dispersed in the presence of excess oleylamine, the nanocrystal surfaces were etched over time (see the Supporting Information). Similar etching of their Cu-In-Se nanocrystals left in TOP/oleylamine for too long was observed by Allen and Bawendi.¹⁶ Guo et al.¹⁷ also reported the formation of hollow CuInSe_2 nanorings when TOP/oleylamine was used as a reaction solvent. Therefore, care must be taken when using oleylamine to make CuInSe_2 nanocrystals.

In summary, a new synthetic route to monodisperse chalcopyrite CuInSe_2 nanocrystals was developed in which selenourea, CuCl , and InCl_3 are used as reactants and oleylamine is used as a reaction solvent. The nanocrystals exhibit trigonal pyramidal shape related to the polarity

and stability of the chalcopyrite surface facets. This study shows that monodisperse nanocrystals of compositionally complex ternary compounds can be synthesized by solution routes. Similar approaches will most likely work for other ternary or quaternary compounds, including Cu(In,Ga)Se_2 (CIGS) nanocrystals and $\text{Cu}_2\text{ZnSnSe}_4$ (CZTS) materials that are candidates for new PV devices.

Acknowledgment. This research was supported by funding from the National Science Foundation through their STC program (CHE-9876674), the Robert A. Welch Foundation, and the Air Force Research Laboratory (FA8650-07-2-5061).

Supporting Information Available: Experimental details, SEM and TEM images and XRD and EDS data for CuInSe_2 nanocrystals, crystallographic models of the unit cell and crystal planes of chalcopyrite CuInSe_2 , and TEM and XRD results for oleylamine-etched nanocrystals. This material is available free of charge via the Internet at <http://pubs.acs.org>.

References

- Gur, I.; Fromer, N. A.; Geier, M. L.; Alivisatos, A. P. *Science* **2005**, *310*, 462.
- Wu, Y.; Wadia, C.; Ma, W.; Sadtler, B.; Alivisatos, A. P. *Nano Lett.* **2008**, *8*, 2551.
- Huynh, W. U.; Dittmer, J. J.; Alivisatos, A. P. *Science* **2002**, *295*, 2425.
- Gunes, S.; Neugebauer, H.; Sariciftci, N. S.; Roither, H.; Kovalenko, M.; Pillwein, G.; Heiss, W. *Adv. Funct. Mater.* **2006**, *16*, 1095.
- Leschkles, K. S.; Dlvakar, R.; Basu, J.; Enache-Pommer, E.; Boercker, J. E.; Carter, C. B.; Kortshagen, U. R.; Norris, D. J.; Aydil, E. S. *Nano Lett.* **2007**, *7*, 1793.
- Manna, L.; Milliron, D. J.; Meisel, A.; Scher, E. C.; Alivisatos, A. P. *Nat. Mater.* **2003**, *2*, 382.
- Cho, K.-S.; Talpin, D. V.; Gaschler, W.; Murray, C. B. *J. Am. Chem. Soc.* **2005**, *127*, 7140.
- Lu, X.; Ziegler, K. J.; Ghezlbash, A.; Johnston, K. P.; Korgel, B. A. *Nano Lett.* **2004**, *4*, 969.
- Zhang, X.; Brynda, M.; Britt, R. D.; Carroll, E. C.; Larsen, D. S.; Louie, A. Y.; Kauzlarich, S. M. *J. Am. Chem. Soc.* **2007**, *129*, 10668.
- Yang, Y.-H.; Chen, Y.-T. *J. Phys. Chem. B* **2006**, *110*, 17370.
- Li, B.; Xie, Y.; Huang, J.; Qian, Y. *Adv. Mater.* **1999**, *11*, 1456.
- Gou, X.; Cheng, F.; Shi, Y.; Zhang, L.; Peng, S.; Chen, J.; Shen, P. *J. Am. Chem. Soc.* **2006**, *128*, 7222.
- Castro, S. L.; Bailey, S. G.; Raffaele, R. P.; Banger, K. K.; Hepp, A. F. *Chem. Mater.* **2003**, *15*, 3142.
- Malik, M. A.; O'Brien, P.; Revaprasadu, N. *Adv. Mater.* **1999**, *11*, 1441.
- Zhong, H.; Li, Y.; Ye, M.; Zhu, Z.; Zhou, Y.; Yang, C.; Li, Y. *Nanotechnology* **2007**, *18*, 025602.
- Allen, P. M.; Bawendi, M. G. *J. Am. Chem. Soc.* **2008**, *130*, 9240.
- Guo, Q.; Kim, S. J.; Kar, M.; Shafarman, W. N.; Birkmire, R. W.; Stach, E. A.; Agrawal, R.; Hillhouse, H. W. *Nano Lett.* **2008**, *8*, 2982.
- Panthani, M. G.; Akhavan, V.; Goodfellow, B.; Schmidtke, J. P.; Dunn, L.; Dodabalapur, A.; Barbara, P. F.; Korgel, B. A. *J. Am. Chem. Soc.* **2008**, *130*, 16770.
- Tang, J.; Hinds, S.; Kelley, S. O.; Sargent, E. H. *Chem. Mater.* **2008**, *20*, 6906.
- Repins, I.; Contreras, M. A.; Egaas, B.; DeHart, C.; Scharf, J.; Perkins, C. L.; To, B.; Noufi, R. *Prog. Photovoltaics* **2008**, *16*, 235.
- The chalcopyrite CuInSe_2 bulk band gap is ~ 1 eV. See: *Copper Indium Diselenide for Photovoltaic Applications*; Coutts, T. J., Kazmerski, L. L., Wagner, S., Eds.; Elsevier: Amsterdam, 1986.
- Manna, L.; Scher, E. C.; Alivisatos, A. P. *J. Am. Chem. Soc.* **2000**, *122*, 12700.
- Manna, L.; Wang, L. W.; Cingolani, R.; Alivisatos, A. P. *J. Phys. Chem. B* **2005**, *109*, 6183.
- Barnard, A. S.; Xu, H. *J. Phys. Chem. C* **2007**, *111*, 18112.
- Asokan, S.; Krueger, K. M.; Colvin, V. L.; Wong, M. S. *Small* **2007**, *3*, 1164.
- Sapra, S.; Poppe, J.; Eychmüller, A. *Small* **2007**, *3*, 1886.
- Sadowski, T.; Ramprasad, R. *Phys. Rev. B* **2007**, *76*, 235310.
- Wang, W.; Banerjee, S.; Jia, S.; Steigerwald, M. L.; Herman, I. P. *Chem. Mater.* **2007**, *19*, 2573.
- Xu, X.; Liu, F.; Yu, K.; Huang, W.; Peng, B.; Wei, W. *ChemPhysChem* **2007**, *8*, 703.
- Lou, W.; Chen, M.; Wang, X.; Liu, W. *J. Phys. Chem. C* **2007**, *111*, 9658.
- Pinna, N.; Weiss, K.; Urban, J.; Pileni, M.-P. *Adv. Mater.* **2001**, *13*, 261.
- Shieh, F.; Saunders, A. E.; Korgel, B. A. *J. Phys. Chem. B* **2005**, *109*, 8538.
- Sigman, M. B.; Ghezlbash, A.; Hanrath, T.; Saunders, A. E.; Lee, F.; Korgel, B. A. *J. Am. Chem. Soc.* **2003**, *125*, 16050.
- Ghezlbash, A.; Korgel, B. A. *Langmuir* **2005**, *21*, 9451.
- Jaffe, J. E.; Zunger, A. *Phys. Rev. B* **2001**, *64*, 241304.
- Zhang, S. B.; Wei, S.-H. *Phys. Rev. B* **2002**, *65*, 081402.

JA8080605